2021 43rd Annual International Conference of the
IEEE Engineering in Medicine & Biology Society (EMBC)
Oct 31 - Nov 4, 2021. Virtual Conference

Modified Regularized Wavelength Average Velocity Estimator for normal excitation setup

Valeria Leon C.[1], Stefano E. Romero[1], Sebastian Merino[1], Eduardo Gonzalez[2] and Benjamin Castaneda[1]

***Abstract*— Crawling Waves Sonoelastography (CWS) is an ultrasound elastography approach for the Shear Waves Speed (SWS) estimation. Several studies show promising results for tissue characterization. The algorithms used to calculate the SWS have been commonly implemented considering an opposing vibration sources to the side of the tissue of interest. However, implementing this mechanical setup has important limitations considering the geometry of the body. For that reason, a propagation from the top to the surface can be useful. Previous estimators such as Phase Derivative have been modified and tested in phantom studies, however, the presences of artifacts limited the performed of the SWS map. In this study, the Regularized Wavelength Average Velocity Estimator (R-WAVE) technique is modified and evaluated (RWm) to be used for normal propagation. The results of heterogeneous simulations and phantoms experiments showed consistent results with the literature (ie: Simulations Max Bias PDm 11.64 % · RWm 10.21 %, Max CNR PDm 37.82 dB · RWm 44.42 dB, Phantom Experiments Max Bias PDm 15.42 % · RWm 13.99 %, Max CNR PDm 24.14 dB · RWm 26.40 dB). The result of this study shows the potential of RWm to characterize the stiffness of the tissue as well as to differentiate tumors on in vivo applications.**

Clinical relevance **This study presents a modification of the regularized shear wave speed estimator based on crawling waves sonoelastography approach for medical tissue analysis. This technique can be used to discriminate benignant from malignant tumors.**

I. INTRODUCTION

Elastography imaging is a set of non-invasive techniques that study the elasticity of a tissue. These techniques are commonly used such as complement to clinical diagnosis. In particular, quantitative-ultrasound approaches are often used for being low-cost technology and for their capability to calculate the stiffness based on the Young's module. Tissue excitation is performed by acoustic radiation force or mechanical vibration. However, the limitation of the former is that the vibration of the tissue depends on thermal effects of the transducer which can be limit to the frequency range and safety condition. For that reason, there is a particular interest in mechanical propagation. Crawling Wave Sonoelastography (CWS), introduced by Zhe Wu *et al.* [1], is a non-invasive, painless, and ambulatory quantitative elastography technique that uses Doppler Mode acquisition modality to estimate shear wave propagation displacement in tissue produced by external sources of vibration. *Ex vivo* and *in vivo* experiments have been performed where bars were used to generate the crawling waves (CrW) by vibrating the sides (parallel setup) or the top of the medium (normal setup) [2]. Several shear wave velocity estimators can be applied to the shear waves propagation, which result in tissue elasticity maps. In particular, Phase Derivative [3], has achieved encouraging results for muscle characterization. However, it presents relevant limitations such as the overestimation at the boundaries or the presence of artifacts distributed in the elasticity map. This has been greatly diminished by the Regularized Wavelength Average Velocity Estimator (R-WAVE) [4]; but it has not been implemented and tested for normal propagation.

For this reason, the contribution of this study is the modification of the R-WAVE estimator (RWm) for its application in normal surface propagation.

*Benjamin Castaneda was supported by the PUCP Research Period Award.

[1]Valeria Leon C., Stefano E. Romero, Sebastian Merino and Benjamin Castaneda are with Laboratorio de Imágenes Médicas, Departamento de Ingeniería, Pontificia Universidad Catolica del Perú, Avenida Universitaria 1801, Lima, Perú. valeria.leon@pucp.pe, castaneda.b@pucp.edu.pe, sromerog@pucp.pe

[2]Eduardo Gonzalez is with Johns Hopkins University, Maryland, USA egonza31@jhmi.edu

II. MATERIALS AND METHOD

A. Crawling Wave Sonoelastography - Normal setup

CWS is an ultrasound elastography technique where two mechanical vibration sources placed at the same distance from the transducer are used to create an interference moving pattern [2] as described in the equation (1):

$$|u_T|^2 = \frac{A_1^2}{r_1^2}e^{(-2\alpha_s r_1)} + \frac{A_2^2}{r_2^2}e^{(-2\alpha_s r_2)} + 2\frac{A_1}{r_1}\frac{A_2}{r_2}e^{[-\alpha_s(r_1+r_2)]}.cos[\Delta\omega t + k_s(r_2 - r_1) + \beta + \phi_0], \quad (1)$$

where A_1 and A_2 are the vibration amplitudes, α_s is the attenuation of the tissue, k_s is the shear wave number, $\Delta\omega$ is the difference between angular vibration frequencies, ϕ_0 is a constant phase term, β is a function of the coordinate system and the location of the vibration sources and r_1 and r_2 are the distance from the sources.

B. Modified Phase Derivative Estimator

Shear wave speed (SWS) map can be calculated using the modified Phase Derivative (PDm) estimator [5] which is described in the equation (2).

$$SWS(x,z) = \frac{2(2\pi(f+\Delta f))T_x)}{\theta'(x)}.M(x,z), \quad (2)$$

where T_x is the pitch of the transducer, $\theta'(x)$ is the local phase gradient and M(x,z) is a geometrical compensation matrix described in the equation (3):

$$M(x,z) = \left(\frac{x-d_2}{\sqrt{(x-d_2)^2+z^2}} - \frac{x-d_1}{\sqrt{(x-d_1)^2+z^2}}\right).\frac{1}{2} \tag{3}$$

The use of the M(x,z) matrix is necessary for the calculation of the SWS since when using a normal propagation, its value varies depending on the depth, so a compensation has to be applied.

C. Modified Regularized Wavelength Average Velocity Estimator

A modified version of R-WAVE is proposed based on the framework of Gonzalez *et al.* [4]. Initially, the weighted average speeds (S_{av}) over time must be calculated. A peak detection algorithm was used to calculated the distance between each peaks of the interference pattern along the width of the crawling wave (Figure 1).

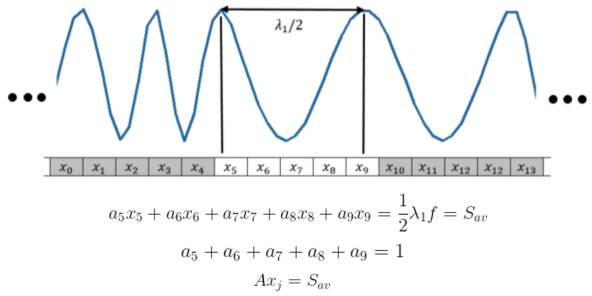

Fig. 1: Interference pattern along the lateral dimension at a selected depth [4]

However, as it was previously described, the SWS in normal propagation changes the wavelength in function of the depth. Then, the following modification is proposed on equation 5:

$$S'_{av} = S_{av}.M(x,z) \tag{4}$$

Therefore, an overdetermined system is generated and solved with the Generalized Tikhonov Regularization approach [6]

$$\hat{x_j} = arg\ min\left[\|Ax_j - S'_{av}\|^2 + \alpha^2 \sum_{i=1}^{N} (|(\Gamma x_j)_i|^2 + \beta)^{\frac{k}{2}}\right], \tag{5}$$

where A is the weighted coefficient matrix map, S'_{av} the modified weighted average speeds and $\hat{x_j}$ the unknown shear wave speeds at depth j, α coefficient of regularization, and Γ the Tikhonov matrix.

D. Simulations

Interference pattern propagation at six different frequencies in the range of 200 Hz to 300 Hz (in 20 Hz steps) were simulated. For each of them, two regions of interest (ROIs) were used for the background (SWS 3.5 m/s) and inclusion (SWS 5.1 m/s, radius 5 mm) of 7.6 mm x 7 mm. The software used to create the simulations was MATLAB 2020a. The pitch and the FR where $3.08e^{-4}$ and 15, respectively, also 1000 axial samples, 337 lateral samples and 68 frames were used for each simulation.

E. Data acquisition

A gelatin-based elasticity phantom of 13 cm x 13 cm x 9 cm with a 5 mm diameter inclusion was excited with two mechanical sources separated 80 mm which were turned upside down and placed at the top of the phantom using rounded head couplings, vibrating at a range of frequencies from 200 to 300 Hz in 20 Hz step. The SWS of the inclusion and the background were estimated to be 5.1 m/s and 3.5 m/s using the time of flight (TOF) test at 20°C. Data was acquired with a SonixTOUCH Research System (Ultrasonix, Richmond, Canada) using a L14-5/38 linear array operating at 6.6 MHz central frequency at a depth of analysis of 4 cm. The SWS were calculated using PDm and RWm. For each estimator, two ROI were taken for the background and inclusion of 10 mm x 10 mm. Two retort stands where used to attach the mechanical sources.

F. Pre-procesing

The color radiofrequency (CRF), data acquired by the ultrasound probe in color doppler mode, is demodulated to obtain in-phase and quadrature signals. The IQ data is then processed using the autocorrelation-based spectral variance estimator proposed by Miller *et al.* [7] to obtain a sonoelasticity video. The estimated variance is normalized along the lateral and temporal axis in order to reduce the noise level.

To enhance the crawling waves Signal-to-Noise Ratio, a 2-D median filter and moving filter were applied [8]. The moving filter consisted of applying the Fourier Transform to each lateral-temporal image, obtaining the energy concentrated in two peaks of known frequency. Then, a band-pass filter is applied based on a stiffness range of 2 - 6 m/s.

III. Results

A. Simulations

Figure 2 shows representative examples of the results where the interference pattern (a), the ideal SWS map (b), the SWS of PDm (c), the SWS of RWm (d), the lateral profile (e) and the axial profile (f) are obtained for a vibration frequency of 200 Hz. The selected ROI of the background is delimited by the two red squares. The ROI of the inclusion is delimited by the black square. The α value for the simulations was 1.2. Additionally, Figure 3 shows the SWS results for the background and the inclusion. A comparison of the SWS is also appreciated with its ideal value for PDm (a) and RWm (b).

The results for background SWS were PDm: 3.19 $\pm$ 0.05 m/s and RWm: 3.18 $\pm$ 0.03 m/s. Likewise, the background coefficients of variation were PDm: 1.57 $\pm$ 0.04 % and RWm: 2.65 $\pm$ 0.21 %. The background bias were PD: 8.66 $\pm$ 1.34 % and RWm: 9.22 $\pm$ 0.82 %. On the other hand,

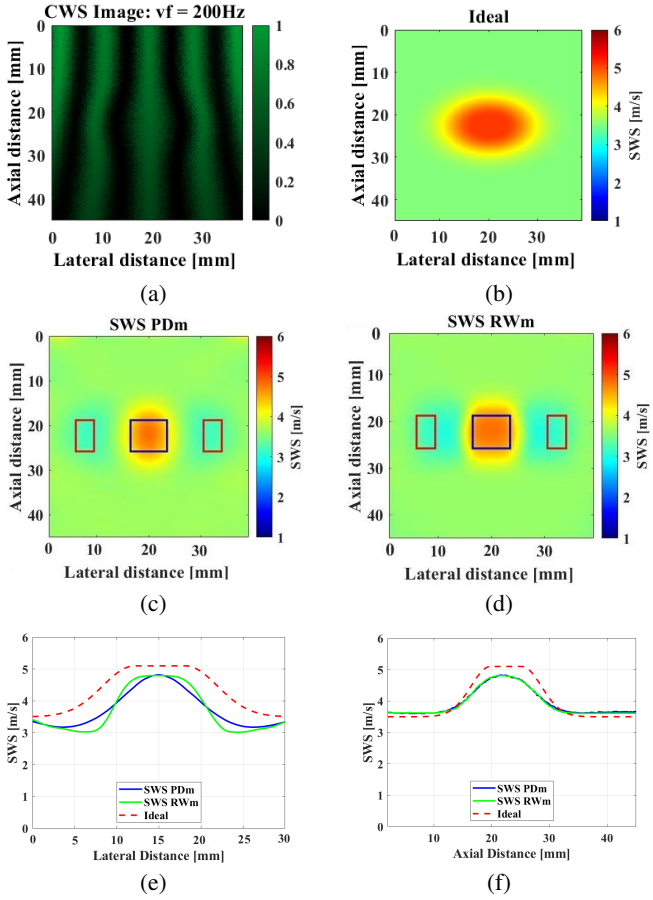

Fig. 2: (a) CWS interference pattern at 200 Hz, (b) Ideal SWS map, (c) SWS PDm map, (d) SWS RWm map, (e) Lateral profile of the center of the SWS map and (f) Axial profile of the center of the SWS map .

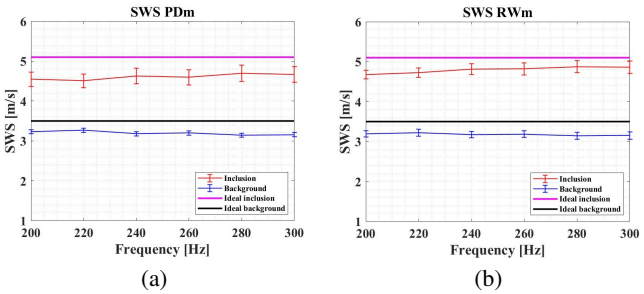

Fig. 3: SWS comparison in the range of 200 Hz to 300 Hz in 20 Hz steps (a) Frequency [Hz] vs. SWS PDm [m/s] (b) Frequency [Hz] vs. SWS RWm [m/s].

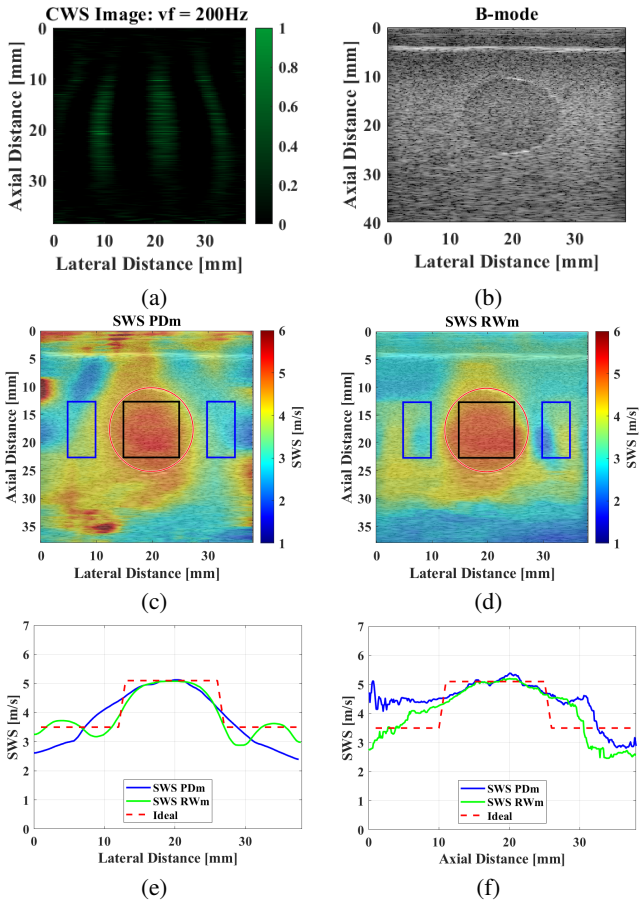

Fig. 4: (a) Interference pattern (b) B-Mode image (c) SWS PDm map (d) SWS RWm map (e) Lateral profile (f) Axial profile.

the resulted inclusion SWS were PDm: 4.48 $\pm$ 0.14 m/s and RWm: 4.61 $\pm$ 0.08 m/s. Likewise, the inclusion coefficients of variation were PDm: 4.12 $\pm$ 0.21 % and RWm: 2.83 $\pm$ 0.35 %. The inclusion bias were PDm: 9.67 $\pm$ 1.42 % and RWm: 5.98 $\pm$ 1.57 %. Additionally, the mean values of the CNR were PD: 37.25 $\pm$ 0.37 dB and RW: 42.11 $\pm$ 1.49 dB.

B. Experiments

Figure 4 shows a representative result of the experiments using 200 Hz. In this case, (a) shows the interference pattern, (b) the B-Mode image, (c) the SWS of PDm, (d) the SWS of RWm, and (e) and (f) the lateral and axial profiles. In the elasticity maps, the shape of the inclusion is shown as a red circle. Similarly, the ROI of the background is delimited by the two blue squares and the ROI of the inclusion is inside the black square. In addition, the results of the SWS for the inclusion and background are observed in Figure 5, the CV and bias results are shown in Figure 6 and the CNR results are shown in Figure 7.

IV. Discussion

The maximum bias and CV for the simulations were 11.64 % and 4.37 %, respectively. This shows that both estimators are quite effective for ideal simulations and can estimate SWS in all the required depth.

According to the physical experiments, RWm generates a good performance in the bias of the background (max: 13%) in contrast with PDm (max: 15%). The CV of the inclusion generates comparative results with an average of 6% in both cases. Similarly, bias and CV of the inclusion generates comparative results both lower than 11%. Figure 6 and Figure 7 show that the RWm estimator has a better

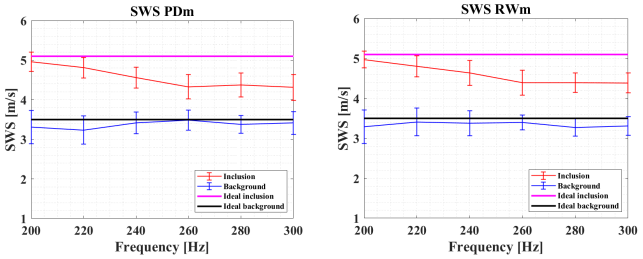

(a) (b)

Fig. 5: SWS comparison in the range of 200 Hz to 300 Hz in 20 Hz steps (a) Frequency [Hz] vs. SWS PDm [m/s] (b) Frequency [Hz] vs. SWS RWm [m/s].

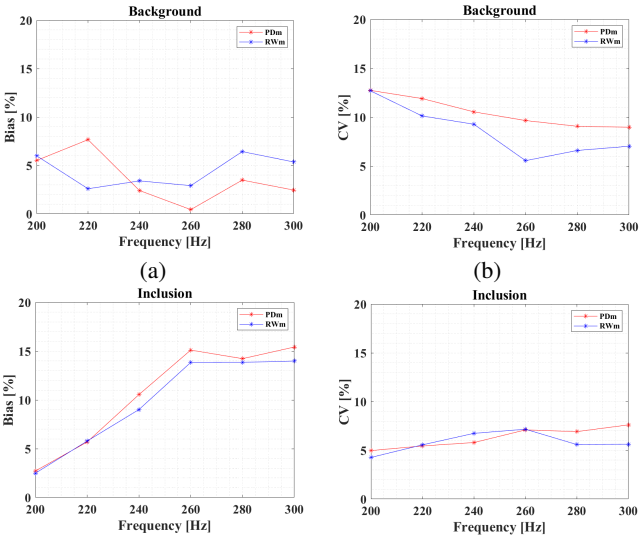

(a) (b) (c) (d)

Fig. 6: Frequency [Hz] vs. bias [%] (a) Background (c) Inclusion. Frequency [Hz] vs. CV [%] (c) Background (d) Inclusion.

performance compared to the PDm estimator. This effect is more noticeable at low frequencies.

In the conventional parallel wave propagation, previous reports mention border artifacts on the SWS estimation using Phase Derivative. Gonzalez *et al.* successfully removed these effects by using the R-WAVE estimator. Similarly, in the normal setup, the artifacts are still present on PDm estimator (Figure 4). Nevertheless, RWm leads to the solution of this problem as well. Also, since RWm works horizontally, the lateral profile in Figure 4 (e) of this estimator shows a clear tendency to the ideal value compared to PDm. Furthermore, in Figure 4 (f), although the PDm and RWm axial profiles present noise components, the RWm one has a better performance in the background due to the use of the median filter. For that reason, it is recommended to create an estimator that works both axially and laterally to obtain a better improvement in this profile.

Finally, a selected range of 2 m/s - 6 m/s in the moving filter was used to overcome the presence of the outliers. However, considering that SWS values change according

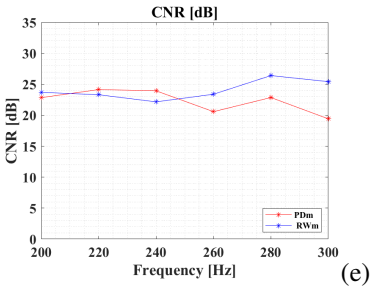

(e)

Fig. 7: Contrast-to-Noise Ratio vs frequency using both estimators in the range of 200 Hz to 300 Hz in 20 Hz steps.

to the depth of the tissue, the moving filter will not have the same performance. Therefore, it would be recommended to use alternative filter approaches that do not depend on possible SWS values.

V. Conclusions and Future Work

A modification of the R-WAVE SWS estimator for normal propagation in CWS was proposed. The performance of the algorithm was compared against PDm estimator providing comparable results in the SWS map reconstruction according to their bias, CV, and CNR. In addition, this approach reduces the previously reported artifacts of PDm. Future work will focus on an estimator that works both axially and laterally, thus avoiding the use of a median filter that deals with the axial non-regularization that is needed in RWm.

Acknowledgment

Benjamin Castaneda was supported by the PUCP Research Period Award.

References

[1] Z. Wu, "Shear wave interferometry and holography, an application of sonoelastography," 2005.

[2] A. Partin, Z. Hah, C. T. Barry, D. J. Rubens, and K. J. Parker, "Elasticity estimates from images of crawling waves generated by miniature surface sources," *Ultrasound in medicine and biology*, vol. 40, no. 4, pp. 685–694, 2014.

[3] Z. Hah, C. Hazard, B. Mills, C. Barry, D. Rubens, and K. Parker, "Integration of crawling waves in an ultrasound imaging system. part 2: signal processing and applications," *Ultrasound in medicine & biology*, vol. 38, no. 2, pp. 312–323, 2012.

[4] E. Gonzalez, Pu Li, J. Ormachea, K. Parker, R. Lavarello, and B. Castaneda, "Regularized wavelength average velocity estimator for quantitative ultrasound elastography," in *2016 IEEE International Ultrasonics Symposium (IUS)*, pp. 1–4, Sep. 2016.

[5] S. E. Romero, E. A. Gonzalez, R. Lavarello, and B. Castañeda, "A comparative study between parallel and normal excitation for crawling wave sonoelastography," in *12th International Symposium on Medical Information Processing and Analysis*, vol. 10160, p. 101601G, International Society for Optics and Photonics, 2017.

[6] R. Lavarello, F. Kamalabadi, and W. D. O'Brien, "A regularized inverse approach to ultrasonic pulse-echo imaging," *IEEE Transactions on Medical Imaging*, vol. 25, no. 6, pp. 712–722, 2006.

[7] K. Miller and M. Rochwarger, "A covariance approach to spectral moment estimation," *IEEE Transactions on Information Theory*, vol. 18, pp. 588–596, Sep. 1972.

[8] B. Castaneda, L. An, S. Wu, L. L. Baxter, J. L. Yao, J. V. Joseph, K. Hoyt, J. Strang, D. J. Rubens, and K. J. Parker, "Prostate cancer detection using crawling wave sonoelastography," in *Medical Imaging 2009: Ultrasonic Imaging and Signal Processing*, vol. 7265, p. 726513, International Society for Optics and Photonics, 2009.